J Therm Anal Calorim (2015) 120:53–58
DOI 10.1007/s10973-014-4228-y

Thermal (kinetic) stability of the inclusion compound on the base of Li-contain MOF $[Li_2(H_2btc)]$·dioxane

Vladimir A. Logvinenko · Sokhrab B. Aliev · Vladimir P. Fedin

Received: 18 April 2014 / Accepted: 3 October 2014 / Published online: 19 October 2014

Abstract The inclusion compounds, based on the metal-organic frameworks (MOFs), have promising practical application in gas storage, separation and fine purification of substances, and also in catalysis. These MOFs are crystalline compounds consisting of metal ions coordinated by bridging organic ligands with the formation of porous structures. We study the kinetic stability of the inclusion compound: $[Li_2(H_2btc)]$·dioxane (H_4btc = 1,2,4,5-benzenetetracarboxylic acid, 1,4–dioxane = $C_4H_8O_2$). The connection between the kinetic stability of inclusion compounds and the properties of the host matrix and of the guest molecules is considered. So as the centrosymmetric dioxane molecule can easily transform the chair conformation to the bath conformation, it can have the influence on the steric hindrance (as well as on the activation barrier) for the guest molecules removal. Therefore, the entropy contribution is as favorable factor, as the energetic one in the kinetic stability of the supramolecular compounds.

Keywords Coordination compounds · Inclusion compounds · Kinetic stability · Metal–organic frameworks · Non-isothermal kinetics · Supramolecular compounds

V. A. Logvinenko (✉) · S. B. Aliev · V. P. Fedin
Nikolaev Institute of Inorganic Chemistry, Siberian Branch of Russian Academy of Sciences, Ac. Lavrentyev Ave 3, Novosibirsk-90 630090, Russia
e-mail: val@niic.nsc.ru

V. A. Logvinenko · V. P. Fedin
Novosibirsk State University, Pirogova St 2, Novosibirsk-90 630090, Russia

Introduction

Metal–organic coordination polymer frameworks (MOFs) are crystalline compounds consisting of metal ions coordinated by bridging organic ligands, which form one-, two-, or three-dimensional structures that can be porous. MOFs with rigid and open skeleton have received intense attention for their potential applications in catalysis, gas storage, molecular recognition, high-capacity adsorbents, non-linear optics, magnetics, and bio-medical imaging. Compared to other porous materials, MOFs provide flexibility in choosing various combinations of linkers and metal, that have different pore sizes, shapes, structures, and functionalities, and can maintain the porous structure for an infinitely long time [1–9]. The advantages of these materials are the simple synthesis process and good thermal stability.

Such MOFs have become a very important topic in hydrogen economics due to their high specific surface areas (500–6,500 $m^2\ g^{-1}$), low densities (0.17–1.7 g cm^{-3}), and tunable pores. The H_2 molecules are linked via van der Waals interactions within the host MOFs. Both experimental and theoretical researches indicated that, owing to the strong affinity of Li^+ for H_2 molecules, H_2 adsorption capacities of MOFs can be significantly enhanced by doping Li^+ into the frameworks [10–19].

The standard process of the MOF production begins from the synthesis of the inclusion compound; the molecules of the used organic solvent (dmf, benzene, thf etc.) are caught in the channels and holes of the metal–organic polymer structure.

These primary included guest molecules are excluded further by the evacuation or by the heating; this process is called the framework activation. Such polymeric matrix with the empty pores (without the support of the included guest molecules) can be thermodynamically or kinetically unstable and collapse, therefore, during the guest molecules moving off. The stability both of the inclusion compound and of the empty framework can be connected with the linker ligand size and structure, or can depend on the structure of the coordination polyhedron [20–22]. Therefore, the quantity estimation of the stability both of the empty host matrix (the activated framework), and of the primary inclusion compound are important for the evaluation and the comparison properties of MOFs in the series.

We study the kinetic stability of the inclusion compound: $[Li_2(H_2btc)]\cdot$dioxane (H_4btc = 1,2,4,5-benzenetetracarboxylic acid, 1,4–dioxane = $C_4H_8O_2$). The another inclusion compound with 1,4–dioxane: $Mn(HCOO)_2\cdot$0.33dioxane was studied earlier [23].

Experimental

The synthesis and the structure study of the inclusion compound $[Li_2(H_2btc)]\cdot$dioxane [24]

The compound was synthesized by the interaction of $LiOH\cdot H_2O$ (10 mg, dissolved in 1.1 cm^3 CH_3OH), 1,2,4,5-benzenetetracarboxylic acid (40 mg), and of 1,4-dioxane (1.1 cm^3) under sonication up to a slurry formation. Colorless octahedral crystals were filtered, washed with 0.5 mL of acetone, and heated at 80 °C during 5 h. Anal: Calc. for $C_{14}H_{12}Li_2O_{10}$ (%): C 47.48; H 3.42. Found (%): C 47.50; H 3.60. Elemental analysis on C and H was performed on a Euro EA 3000 CHN Elemental Analyzer.

Single crystal X-ray diffraction data of $[Li_2(H_2btc)]$ dioxane were collected at 150 K on a Bruker Apex Duo automatic four-circle diffractometer equipped with an area detector (Mo-Kα, $\lambda = 0.71073$ Å, graphite monochromator, φ and ω scans).

The asymmetric unit of $[Li_2(H_2btc)]\cdot$dioxane contains one Li^+ cation and one H_2btc^{2-} anion. Lithium cation has tetrahedral coordination environment. Each Li^+ coordinates four oxygen atoms of four H_2btc^{2-} ligands. The Li–O bond lengths [1.997(2) and 1.8798(19) Å] found fall within the common values for tetrahedral carboxylate complexes of lithium. The lithium cations are interconnected via bridging bidentate μ_2-RCOO–O,O' groups. Consequently, each H_2btc^{2-} anion coordinates eight Li^+ cations forming 3D metal–organic framework. Two carboxylate hydrogen atoms are disordered over all four carboxylic groups of H_2btc^{2-} anion. There are intramolecular hydrogen bonds between neighboring carboxylate groups of H_2btc^{2-} ligand. The metal-organic framework forms square channels (5 × 5 Å) running along the *c*-axis occupied by highly disordered guest 1,4-dioxane molecules that could not be modeled as a set of discrete atomic sites. PLATON/SQUEEZE procedure was employed to calculate the contribution to the diffraction from the solvent region and thereby produced a set of solvent-free diffraction intensities. The final formula of $[Li_2(H_2btc)]\cdot$dioxane was calculated from the SQUEEZE results (388 *e* per unit cell) combined with elemental (C, H) analysis data.

Thermal analysis

TG measurements were carried out on a Netzsch thermal analyser TG 209 F1. The experiments were performed under a helium flow (60 cm^3 min^{-1}) at heating rates of 3, 5, 10, 20, and 40 K min^{-1}. The sample mass was kept cca 5.0 mg.

Kinetic analysis under non-isothermal conditions

Thermogravimetric data were processed with the computer program Netzsch Thermokinetics 2 (Version 2004.05) [25, 26]. A special program module, "Model-free", based on well-known studies [27–33], allows one to process multiple thermogravimetric curves obtained with different heating rates and calculate the activation energy without preliminary information about the kinetic topochemical equation. The Friedman method was used to calculate the activation energies for each experimental point of fractional conversion (in the range $0.005 < \alpha < 0.995$).

If the activation energy is variable in compliance with the Friedman method, therefore, the decomposition process is the multi-stage reaction.

We further used the same set of experimental data to search for the corresponding topochemical equation (the selection was made from 16 equations: chemical reaction at the interface, nucleation, and diffusion). This calculation was made by the improved differential procedure of Borchardt–Daniels within the multiple linear regression approach. It is very important that the range for the degree of conversion (α) for this calculation be chosen based on the relative constancy of the calculated kinetic parameters from the Friedman analysis.

The F test [25] was used to search for the best kinetic description and for statistical control of the obtained equation. It tests the residual variance of individual models against one another and answers the question of whether the models differ significantly (statistically) or not. If $F_{exp(1)} \approx F_{exp(2)}$ for two equations, there is no reason to assume the first model is better at characterizing the experiment. The statistical quantile F_{crit} is obtained for a level of significance of 0.05.

If the calculation results in two or three kinetic equations with close values in their correlation coefficients and on the F_{test}, but with noticeably different values in kinetics parameters, it is most correct to choose the equation with activation energy values closest to the data from the

"Model-free" module program. Discrimination between the two steps is very relative in this search for topochemical equations, but it helps to find the most reliable ones. The special program of non-linear regression is useful in searching for a full set of kinetic parameters for multi-stage processes. The closest fit between the activation energies from the ''Model-free'' analysis and the non-linear regression calculation is important from a physicochemical point of view. Therefore, the authors of the computer program used recommend fixing *E* values (obtained by linear regression and congruent with *E* from the ''Model-free'' analysis) in calculations with this program.

The random error in the activation energy values for such a reversible decomposition reaction is usually about 10 % in these experiments, which we took into consideration. The computer program Netzsch Thermokinetics 2 enables estimation of the contribution of each stage (as Δm portion) after this non-linear regression calculation.

New studies on non-isothermal kinetics were taken into account [34–37]; well-known recommendations for performing kinetic computations on thermal analysis data [38] were used.

There were several important assumptions and limitations. The kinetic equations to calculate the kinetic parameters are topochemical ones and the calculated parameters (*E* and *A*) are formal and conventional from the standpoint of the classical chemistry of solids.

However, the general trend in the variation of these values within a specially selected series of compounds (either isostructural or genetically related) is very important because the expected disorder in the reaction zones can be identical for them; all other errors will be minimized and smoothed in such a comparison. The best series are the coordination compounds with volatile ligands (with one central atom and different ligands or with different central atoms and the same ligand) or the inclusion compounds (with the same host matrix and the different guest molecules) [39–46].

The rate constant (*k*) and the pre-exponential factor (*A*) were calculated in sec^{-1}.

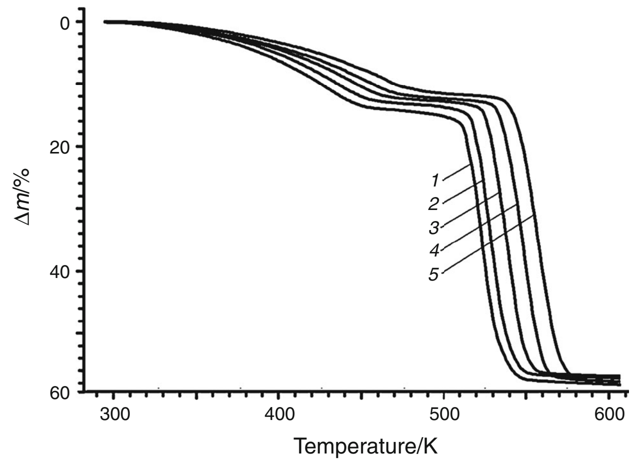

Fig. 1 Thermal decomposition of $[Li_2(H_2btc)]\cdot$dioxane. Sample mass cca. 5 mg; helium flow 60 $cm^3\ min^{-1}$. The heating rates were 3 (*1*), 5 (*2*), 10 (*3*) 20 (*4*) and 40 (*5*) K min^{-1}. The first step is the inclusion compound decomposition; the second step is the host matrix destruction

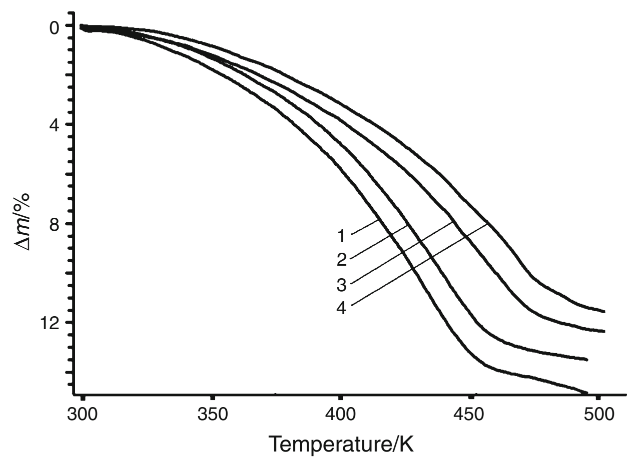

Fig. 2 Thermal decomposition of $[Li_2(H_2btc)]\cdot$dioxane, TG curves corresponding to the first mass loss step (Fig. 1). Sample mass cca 5 mg; helium flow 60 $cm^3\ min^{-1}$. The heating rates were 3 (*1*), 5 (*2*), 20 (*3*) and 40 (*4*) K min^{-1}

Results and discussion

The inclusion compound $[Li_2(H_2btc)]\cdot$dioxane decomposes in two well-defined steps (Fig. 1). The first step is the guest molecules removal; the more is the heating rate, the less is the dioxane removal before host matrix destruction. The half of the included dioxane (12–14 % from 24.9 %) is removed at experimental conditions. MOF structure distorts during guest molecules removal and the residual dioxane molecules get stuck in the collapsed channels. The whole mass loss at 600 K after the full pyrolysis is the same for all experiments with different heating rates.

The only way the inclusion compound can lose all included dioxane without the framework collapse is vacuum pumping during several days at 90 °C.

The decomposition step at 300–500 K (Fig. 1) was chosen for the kinetic study; it corresponds to the dioxane removal: $[Li_2(H_2btc)]\cdot$dioxane → $[Li_2(H_2btc)]\cdot(1–n)$ dioxane + *n* dioxane↑ (Fig. 2).

''Model–free'' data are given in Fig. 3. The activation energy can be considered as variable in compliance with

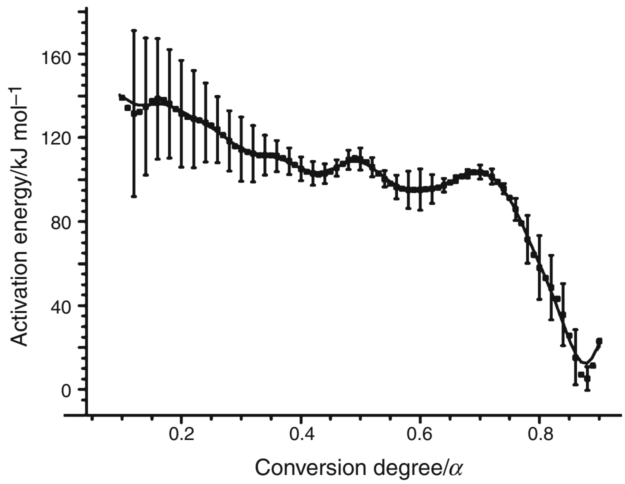

Fig. 3 Friedman analysis of $[Li_2(H_2btc)]$·dioxane thermal decomposition: activation energies depending on the degree of conversion α. *Perpendicular lines* SD of calculation

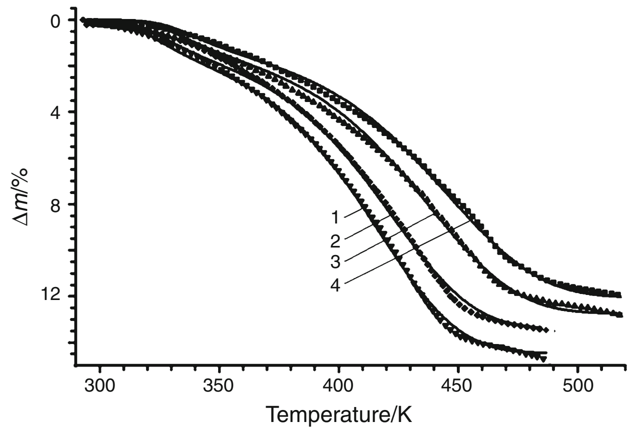

Fig. 4 Data processing for thermal decomposition $[Li_2(H_2btc)]$·dioxane. TG *curves* fitting of non-linear regression, simulated with two consecutive (A → B → C) reactions (equations Fn and An). The heating rates were 3 (*1*), 5 (*2*), 20 (*3*) and 40(*4*) K min^{-1}. The *points* are the experimental data; the *lines* are the calculated data

Table 1 $[Li_2(H_2btc)]$·(dioxane) decomposition

F_{crit}	F_{exp}	F_{act}	Equation A → B	Equation B → C	Equation C → D
1.09	1.00	1489	An		An
1.09	1.35	1489	Fn		An
1.09	1.50	1489	Fn	An	
1.09	1.60	1489	An	Fn	
1.09	3.20	1489	Fn	Fn	
1.09	3.36	1489	An	B1	
1.09	5.57	1489	An	An	

The used topochemical equations are Avrami-Erofeev (An), *n*-th order (Fn) and Prout-Tompkins (B1) equations [25, 26]. Data on the *F* test of fit quality/to identify the best kinetic description/

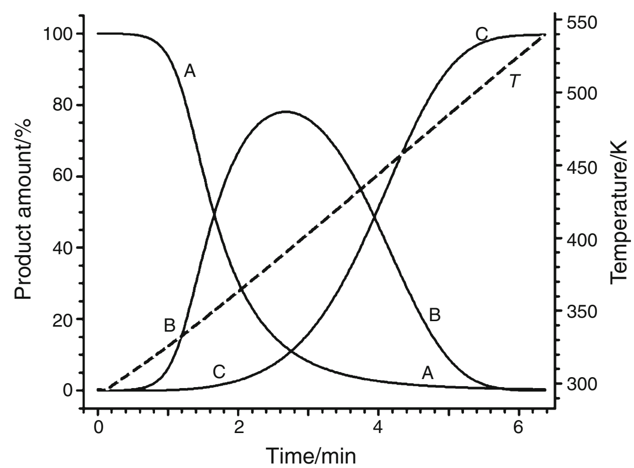

Fig. 5 Thermal decomposition of $[Li_2(H_2btc)]$·dioxane. Time dependence of the yield for each reactant in the decomposition. The calculation corresponds to two-stage consecutive processes (A → B → C) in Fig. 4. The heating rate is 40 K min^{-1}

the Friedman method; therefore, the decomposition process is the multi-stage reaction. The best descriptions for the process are the two-stage processes: or with the concurrent reactions (A → B; C → D), or with the consecutive ones (A → B → C), with the *n*-order equation (Fn) and the Avrami–Erofeev equation (An) for the stages (Table 1).

The most probable estimate is two consecutive reactions (Fig. 4):

A → B Fn, $f_1(\alpha) = (1–\alpha)^{4.8}$, $E_1 = 148 \pm 9$ kJ mol^{-1}, lg $A_1 = 22 \pm 1$.

B → C An, $f_2(\alpha) = (1–\alpha)/[–\ln(1–\alpha)]^{1.7}$, $E_1 = 132 \pm 2$ kJ mol^{-1}, lg $A_2 = 13.9 \pm 0.2$.

Corr. coeff. = 0.999393. The time dependencies of the yield for each reactant in the decomposition are shown in Fig. 5. The mentioned mass loss step $\Delta m \approx 12–14$ % is related to ≈0.5 dioxane molecule removal. The used computer program enables estimation of the contribution of each stage (as Δm portion) after the non-linear regression calculation. If 0.5 dioxane molecule removal is related to 100 % of this step of decomposition, the first stage (A → B) corresponds to 14.9 %, the second stage (B → C) corresponds to 85.1 % of this decomposition step. The approximate composition of the intermediate phase (B) is $[Li_2(H_2btc)]$·0.4(dioxane), it is kinetically hindered metastable phase.

The order *n* in Fn equation is big; the dispersion of the particles is considered usually as a reason for the experimental order increase [47].

The Avrami–Erofeev equations describe the main decomposition part; the equation form indicates the evident diffusion contribution.

Conclusions

The interaction between the guest molecules and the framework in such supramolecular compounds is generally due to van der Waals forces. It is worth to compare the thermal (kinetic) stability of two different inclusion compounds with the same 1,4–dioxane guest molecules:

$$Mn(HCOO)_2{\cdot}0.33C_4H_8O_2 \rightarrow Mn(HCOO)_2 + 0.33C_4H_8O_2\uparrow$$

The temperature interval of the decomposition is 470–540 K; E_a = 78 kJ mol^{-1}; lg A_a = 6.3 [23].

$$[Li_2(H_2btc)] \cdot nC_4H_8O_2 \rightarrow [Li_2(H_2btc)] \cdot 0.5C_4H_8O_2 + 0,5C_4H_8O_2\uparrow$$

The temperature interval of the decomposition is 300–500 K; E_b = 148 kJ mol^{-1}; lg A_b = 22.

The unusual difference between the kinetic stability ($T_{a\ init} > T_{b\ init}$, but $E_a < E_b$) can be connected with the different channels structures and the different flexibilities of the host matrices. $Mn(HCOO)_2{\cdot}0.33C_4H_8O_2$ structure encloses adamantane-like cages (with an internal diameter of 5.5 Å); they are connected to each other via small window of 4.5 Å to form a 1D zigzag channel along the *b*-axis [48]. It was shown that this structure expands during the heating in the temperature interval 30–200 °C and begins to decompose only after this phase transition [23, 41]; dioxane molecules leave the expanded channels rather easily. It seems that the more rigid $[Li_2(H_2btc)]$ structure does not expand before the decomposition.

The initial temperatures of two compounds thermal decomposition (≈470 and ≈300 K) at the same experimental conditions (10 K min^{-1}) are the temperatures of the achievement of the identical (one and the same) rate constant [39, 40]. Therefore, $Mn(HCOO)_2{\cdot}0.33$dioxane compound is more stable, if we compare the kinetic stability by the rate constants. But this high stability depends not on the activation energy value (it is small: E_a = 78 kJ mol^{-1}), but on the very low value of the pre-exponential factor ($A_a = 10^{6.3}$ s^{-1}). Therefore, the great difference in the kinetic stability for these two inclusion compounds with the dioxane depends a lot more on the entropy factor.

One can take into account that the centrosymmetric 1, 4–dioxane molecule has the chair conformation, but easily transforms to the bath conformation. It will change the steric hindrance (as well as the activation barrier) for the guest molecules removal at the difference temperature intervals through the different channels configurations.

It is an additional proof that the entropy contribution is as favorable factor, as the energetic one in the kinetic stability of the supramolecular compounds [41, 43].

Acknowledgements The work was partially supported by the Grant of the Government of the Russian Federation (GN 14.Z50.31.0006).

References

1. Fromm KM. Coordination polymer networks with s-block metal ions. Coord Chem Rev. 2008;252:856–85.
2. Kirillov AM. Hexamethylenetetramine: an old new building block for design of coordination polymers. Coord Chem Rev. 2011;255:1603–22.
3. Mani–Biswas M, Tahir Cagin T. Insights from theoretical calculations on structure, dynamics, phase behavior and hydrogen sorption in nanoporous metal organic frameworks. Comput Theor Chem. 2012;987:42–56.
4. Lyszczek R, Iwan M. Investigation of desolvation process in lanthanide dinicotinates, J. Therm Anal Calorim. 2011;103: 633–9.
5. Jiang C-H, Song LF, Jiao CL, Zhang J, Sun LX, Xu F, Du Y, Cao Z. Exceptional thermal stability and thermodynamic properties of lithium based metal-organic framework. J Therm Anal Calorim. 2011;103:373–80.
6. Zhou YZ, Sun LX, Cao Z, Zhang J, Xu F, Song LF, Zhao ZM, Zou YJ. Heat capacities and thermodynamic properties M(HBTC)(4, 4′-bipy)·3DMF (M = Ni and Co). J Therm Anal Calorim. 2012;110:949–54.
7. Dybtsev DN, Yutkin MP, Peresypkina EV, Virovets AV, Serre C, Ferey G, Fedin VP. Isoreticular homochiral porous metal–organic structures with tunable pore sizes. Inorg Chem. 2007;46:6843–5.
8. Dybtsev DN, Yutkin MP, Samsonenko DG, Fedin VP, Nuzhdin AL, Bezrukov AA, Bryliakov RP, Talsi EP, Belosludov RV, Mizuseki H, Kawazoe Y, Subbotin OS, Belosludov VR. Modular homochiral porous coordination polymers: rational design, enantioselective guest exchange sorption and ab initio calculations of host-guest interactions. Chem Eur J. 2010;10:348–56.
9. Yin Z, Zeng MH. Recent advance in porous coordination polymers from the view-point of crystalline-state transformation. Sci China Chem. 2011;54:1371–94.
10. Eddaoudi M, Li H, Reineke T, Fehr M, Kelley D, Groy TL, Yaghi OM. Design and synthesis of metal-organic frameworks with permanent microporosity. Top Catal. 1999;105:105–11.
11. Rowsell JLC, Yaghi OM. Strategies for hydrogen storage in metal-organic frameworks. Angew Chem Int Ed. 2005;44:4670–9.
12. Zhao D, Yuan DQ, Zhou HC. The current status of hydrogen storage in metal-organic frameworks. Energ Env Sci. 2008;1: 222–35.
13. Combelles C, Doublet ML. Structural, magnetic and redox properties of a new cathode material for Li-ion batteries: the iron-based metal organic framework. Ionics. 2008;14:279–83.
14. Murray LJ, Dinca M, Long JR. Hydrogen storage in metalorganic frameworks. Chem Soc Rev. 2009;38:1294–314.
15. Xiang ZH, Cao DP, Lan JH, Wang WC, Broom DP. Multiscale simulation and modelling of adsorptive processes for energy gas storage and carbon dioxide capture in porous coordination frameworks. Energ Env Sci. 2010;3:1469–87.

16. Maark TA, Pal S. A model study of effect of M = Li^+, Na^+, Be^{2+}, Mg^{2+}, and Al^{3+} ion decoration on hydrogen adsorption of metal-organic framework. Int J Hydrog Energ. 2010;535: 12846–57.
17. Dixit M, Maark AT, Pal S. Ab initio and periodic DFT investigation of hydrogen storage on light metal-decorated MOF-5. Int J Hydrog Energ. 2011;36:10816–27.
18. Combelles C, Yahia MB, Pedesseau L, Doublet ML. FeII/FeIII mixed-valence state induced by Li-insertion into the metal-organic-framework Mil53(Fe): a DFT + U study. J Power Sourc. 2011;196:3426–32.
19. Xiang Z, Hu Z, Yang W, Cao D. Lithium doping H_2 storage. Int J Hydrog Energ. 2012;37:946–50.
20. YuA Dyadin, Soldatov DV, Logvinenko VA, Lipkovsky J. Contact stabilization of host complex molecules during clathrate formation: the pyridine–zinc nitrate and the pyridine–cadmium nitrate systems. J Coord Chem. 1996;37:63–75.
21. Logvinenko V, Dybtsev D, Fedin V, Drebushchak V, Yutkin M. The stability of inclusion compounds under heating. Part 2. The stability of inclusion compounds of layered zinc camphorate, linked by linear N-donor ligands. J Therm Anal Calorim. 2010;100:183–9.
22. Logvinenko VA, Yutkin MP, Zavakhina MS, Fedin VP. Porous metal-organic frameworks (MOFs) as matrices for inclusion compounds. Kinetic stability under heating. J Therm Anal Calorim. 2012;109:555–60.
23. Logvinenko V, Dybtsev D, Fedin V, Drebushchak V, Yutkin M. The stability of inclusion compounds under heating. Part I. Inclusion compounds of micro-porous manganese formate with included dioxane Mn(HCOO)2·1/3C4H8O2 and tetra- hydrofurane {Mn(HCOO)2·1/3C4H8O}. J. Therm Anal Calorim. 2007;90:463–7.
24. Aliev SB, Samsonenko DG, Rakhmanova MI, Dybtsev DN, Fedin VP. Syntheses and structural characterization of lithium carboxylate frameworks and guest-dependent photoluminescence study. Cryst Growth Des. 2014;14:4355–63.
25. Netzsch thermokinetics. http://www.netzsch-thermal-analysis.com/us/thermokinetics-workshop.
26. Moukhina E. Determination of kinetic mechanisms for reactions measured with thermoanalytical instruments. J Therm Anal Calorim. 2012;109:1203–14.
27. Kissinger HE. Reaction kinetics in differential thermal analysis. Anal Chem. 1957;29:1702–6.
28. Friedman HL. Kinetics of thermal degradation of char-forming plastics from thermogravimetry. J Polym Sci. 1963;6:183–95.
29. Ozawa T. Estimation of activation energy by isoconversion methods. Thermochim Acta. 1992;203:159–65.
30. Flynn JH, Wall LA. General treatment of the thermogravimetry of polymers. J Res Nat Bur Stand. 1966;70:478–523.
31. Opfermann J, Kaisersberger E. An advantageous variant of the Ozawa-Flynn-Wall analysis. Thermochim Acta. 1992;203:167–75.
32. Opferman JR, Kaisersberger E, Flammersheim HJ. Model-free analysis of thermo- analytical data-advantages and limitations. Thermochim Acta. 2001;391:119–27.
33. Vyazovkin S. Model-free kinetics: staying free of multiplying entities without necessity. J Therm Anal Calorim. 2006;83:45–51.
34. Simon P. Single-step kinetics approximation employing nonarrhenius temperature functions. J Therm Anal Calorim. 2005;79: 703–8.
35. Simon P. The single-step approximation: attributes, strong and weak sides. J Therm Anal Calorim. 2007;88:709–15.
36. Simon P, Thomas P, Dubaj T, Cibulkova Z, Peller A, Veverka M. The mathematical incorrectness of the integral isoconversional methods in case of variable activation energy and the consequences. J Therm Anal Calorim. 2014;115:853–9.
37. Sestak J. Is the original Kissinger equation obsolete today: not obsolete the entire non- isothermal kinetics? J Therm Anal Calorim. 2014;117:3–7.
38. Vyazovkin S, Burnham AK, Criado JM, Luis A, Perez-Maqueda LA, Popescu C, Sbirrazzuoli N. ICTAC kinetics committee recommendations for performing kinetic computations on thermal analysis data. Thermochim Acta. 2011;520:1–19.
39. Logvinenko V. Stability and reactivity of coordination and inclusion compounds in the reversible processes of thermal dissociation. Thermochim Acta. 1999;340:293–9.
40. Logvinenko V. Solid state coordination chemistry. The quantitative thermoanalytical study of thermal dissociation reactions. J Therm Anal Calorim. 2000;60:9–15.
41. Logvinenko V. Stability of supramolecular compounds under heating. Thermodynamic and kinetic aspects. J Therm Anal Calorim. 2010;101:577–83.
42. Logvinenko V, Fedorov V, Mironov Y, Drebushchak V. Kinetic and thermodynamic stability of cluster compounds under heating. J Therm Anal. 2007;88:687–92.
43. Logvinenko V, Drebushchak V, Pinakov D, Chekhova G. Thermodynamic and kinetic stability of inclusion compounds under heating. J Therm Anal. 2007;90:23–30.
44. Pinakov DV, Logvinenko VA, Chekhova GN, Shubin YuV. The relationship between properties of fluorinated graphite intercalates and matrix composition. Part VI. J Therm Anal Calorim. 2014;115:503–9.
45. Logvinenko VA, Belyaev AV, Vorob'eva SN. Dehydration process of rhodium sulfate crystalline hydrate. J Therm Anal Calorim. 2013;114:1177–81.
46. Logvinenko V, Bakovets V, Trushnikova L. Dehydroxylation kinetics of gadolinium hydroxide. J Therm Anal Calorim. 2014;115:517–21.
47. Delmon B, Introduction a la cinetique heterogene. Editions Technip, 7 Rue Nelaton. Paris 15^0, 1969.
48. Dybtsev DN, Chun H, Yoon SH, Kim D, Kim K. Microporous manganese formate: a simple metal-organic porous material with high framework stability and highly selective gas sorption properties. J Am Chem Soc. 2004;126:32–3.